

Synthesis and Characterization of Polyoxovanadate-Pillared Zn–Al Layered Double Hydroxides: An X-ray Absorption and Diffraction Study

C. Barriga,[†] W. Jones,[‡] P. Malet,[§] V. Rives,^{||} and M. A. Ulibarri^{*,†}

Departamento de Química Inorgánica e Ingeniería Química, Facultad de Ciencias, Universidad de Córdoba, 14004-Córdoba, Spain, Department of Chemistry, University of Cambridge, Lensfield Road, Cambridge CB2 1EW, England, Departamento de Química Inorgánica e Instituto de Ciencia de Materiales, Universidad de Sevilla-CSIC, Sevilla, Spain, and Departamento de Química Inorgánica, Universidad de Salamanca, 37007-Salamanca, Spain

Received July 24, 1997

Zn–Al layered double hydroxides (LDHs) have been prepared with Cl^- and CO_3^{2-} interlayer anions and with Zn/Al ratios of 2 and 3. The corresponding polyoxovanadate-containing LDHs were then prepared by anion exchange reaction at different pH values. The products were characterized by atomic absorption, PXRD, FT-IR spectroscopy, TG analysis, and transmission electron microscopy (TEM). The resulting vanadate-containing LDHs, depending on the pH and the Zn/Al ratio, consisted of one or more phases. PXRD patterns corresponding to layered compounds with different gallery heights (7.0, 4.6, and 2.6 Å for $\text{V}_{10}\text{O}_{28}^{6-}$, $\text{V}_4\text{O}_{12}^{4-}$ and $(\text{VO}_3)_n^{n-}$ chains, respectively) were observed. X-ray absorption spectroscopy has been also used to assess the local geometry of vanadium ions in the different samples, and results indicate the presence of V^{5+} ions in octahedral and/or tetrahedral coordination depending upon the conditions of the synthesis.

Introduction

Layered double hydroxides (LDHs) have the general formula $[\text{M}^{\text{II}}_{1-x}\text{M}^{\text{III}}_x(\text{OH})_2]^{x+}\text{A}_{x/z}^{z-}\cdot n\text{H}_2\text{O}$ and consist of brucite-like layers, $\text{Mg}(\text{OH})_2$, in which divalent cations are partially substituted for trivalent ones. The layers, as a result, carry a positive charge, which is balanced by interlayer anions. Accompanying the anions are variable amounts of interlayer water.

Such LDHs may be used as precursors of pillared layered structures (PLSs). An important feature of PLSs is that they can be tailor-made, whether by modification of the host structure chemical composition or by chemical or structural modification of the guest species domains. They show a broad range of structural, chemical, electronic, ionic, optical, and magnetic applications.¹ To prove the chemical and physical properties of these compounds, it is important to obtain information concerning the local environment of the metallic cations. As a result several studies have been described concerning their synthesis, characterization, and structure.^{1–6} Among the different anions used as precursors of the interlayer pillars, decavanadate, $\text{V}_{10}\text{O}_{28}^{6-}$, is probably one of the widest studied, because of the stability of its structure and also because of the interest as catalysts of the mixed oxides obtained upon its thermal decomposition.³

Several methods have been used to synthesize LDHs intercalated with polyoxovanadate anions: direct synthesis,^{4,5} ex-

change of chloride or nitrate anions,⁶ swelling with a large organic anion, which is subsequently displaced by polyoxovanadate species,^{7–9} and calcination of LDHs and recovering (reconstruction) of a layered structure with polyoxovanadate,^{7,10} by means of the so-called “memory effect”.

The aim of the present work is to prepare Zn–Al LDHs of different Zn/Al ratios with Cl^- or CO_3^{2-} in the interlayer space, to be used as precursors for decavanadate-containing LDHs. The exchange ability of interlayer anions depends both on their formal charge (monovalent anions are more readily exchanged than divalent ones) and on their intrinsic nature (carbonate is strongly held).² Polymerization of oxovanadate is pH-sensitive, and as a result, changes in the pH are expected to lead to species with different polymerization degrees incorporated into the interlayer region. The products have been characterized using several complementary experimental techniques. In particular, XAS spectroscopies have been also applied to assess the local environment around the vanadium ions, as differences are expected for different vanadate species.

Experimental Section

Synthesis of Parent Materials. The parent LDHs were prepared with chloride or carbonate in the interlayer and with Zn/Al ratios 2 and 3.

(a) Chloride-Containing Zn–Al LDHs. The coprecipitation method was followed, and low metal salt concentrations were used in

* To whom correspondence should be addressed. Fax: +34 57 21 86 06. E-mail: iq1ulcom@uco.es.

[†] Universidad de Córdoba.

[‡] University of Cambridge.

[§] Universidad de Sevilla-CSIC.

^{||} Universidad de Salamanca.

- (1) De Roy, A.; Forano C.; Malki K. E.; Besse, J. P. In *Synthesis of Microporous Materials VII*; Occelli, M. O., Robson, M. E., Eds.; Van Nostrand: New York, 1992; p 108.
- (2) Cavani, F.; Trifiró, F.; Vaccari, A. *Catal. Today* **1991**, *11*, 73.
- (3) Doeuff, M.; Kwon, T.; Pinnavaia, T. J. *Synth. Met.* **1989**, *34*, 609.

- (4) Kooli, F.; Jones, W. *Inorg. Chem.* **1995**, *34*, 6237.

- (5) Narita, E.; Kaviratna, P. D.; Pinnavaia T. J. *J. Chem. Soc., Chem. Commun.* **1993**, 60.

- (6) (a) Kooli, F.; Rives, V.; Ulibarri M. A. *Inorg. Chem.* **1995**, *34*, 5114.

- (b) Kooli, F.; Rives, V.; Ulibarri, M. A. *Inorg. Chem.* **1995**, *34*, 5120.

- (7) Ulibarri, M. A.; Labajos, F. M.; Rives, V.; Trujillano, R.; Kagunya, W.; Jones, W. *Inorg. Chem.* **1994**, *33*, 2592.

- (8) Dimotakis, E. D.; Pinnavaia, T. J. *Inorg. Chem.* **1990**, *29*, 2393.

- (9) Drezdon, M. A. *Inorg. Chem.* **1988**, *27*, 4628.

- (10) Narita, E.; Kaviratna, P.; Pinnavaia, T. J. *Chem. Lett.* **1991**, 805.

order to avoid precipitation of ZnO. A solution (200 mL) containing ZnCl_2 and $\text{AlCl}_3 \cdot 6\text{H}_2\text{O}$ ($[\text{Zn}^{\text{II}} + \text{Al}^{\text{III}}] = 0.04 \text{ M}$) was added dropwise to 50 mL of water at room temperature, the pH being adjusted to 8 by using aqueous NaOH (0.5 M). Once the addition was complete, the mixture was stirred for 2 h with the reaction mixture purged with N_2 to avoid carbon dioxide uptake. The products were separated by centrifugation, washed, and dried under vacuum at room temperature.

(b) Carbonate-Containing Zn–Al LDHs. The coprecipitation method was again used. A solution (100 mL) containing $\text{Zn}(\text{NO}_3)_2 \cdot 6\text{H}_2\text{O}$ and $\text{Al}(\text{NO}_3)_3 \cdot 9\text{H}_2\text{O}$ ($[\text{Zn}^{\text{II}} + \text{Al}^{\text{III}}] = 0.3 \text{ M}$) was added with vigorous stirring to a solution (100 mL) of 1 M Na_2CO_3 . The addition was over 3 h, and the mixture was kept at 60 °C. The pH was maintained at a value of 10 with a pH-stat apparatus. The resulting slurry was centrifuged and washed several times with distilled water with the solids being dried in an oven at 60 °C.

The parent carbonate and chloride samples are designated ZnXAlY , where X stands for the nominal Zn/Al atomic ratio and Y for the interlayer anion, i.e., Zn_2AlCl , Zn_3AlCl , Zn_2AlCO_3 , and Zn_3AlCO_3 .

Synthesis of Polyoxovanadate-Pillared LDHs. In all cases, the polyoxovanadate-containing samples were prepared by ion exchange from parent chloride- or carbonate-containing samples.

(a) Anion Exchange of Chloride Zn–Al LDHs. A fresh slurry (30 mL, containing 0.5 g of solid) of Zn_2AlCl or Zn_3AlCl samples was stirred for 15 min at room temperature. The pH of the slurry was adjusted to 4, 5, 6, or 7 with HCl (0.5 M) solution. A 50 mL volume of a 0.1 M aqueous solution of NaVO_3 was then added dropwise to the slurry. Formation of gel was not observed. During addition, nitrogen was bubbled through the suspension with the pH maintained at the constant preset value and the temperature at 40 °C. The mixture was then stirred overnight at room temperature (without continued nitrogen flow) and submitted to hydrothermal treatment at 90 °C for 18 h in a stainless steel bomb lined with Teflon. The yellow-orange precipitate was washed with deionized, carbonate-free water and dried at 50 °C. Elemental chemical analysis showed the absence of chloride in these solids. These samples are designated ZnXAlVY , where X stands for the nominal Zn/Al atomic ratio in the parent material and Y for the pH at which exchange took place.

(b) Anion Exchange of Carbonate Zn–Al LDHs. A 50 mL volume of a 0.1 M aqueous suspension of NaVO_3 (the pH of which had been previously adjusted to 4.5 with 0.5 M HCl) was added to 100 mL of a suspension containing 1 g of Zn_2AlCO_3 or Zn_3AlCO_3 at 60 °C. The slurry was magnetically stirred for 2 h, while the pH was maintained at the preset value of 4.5. The samples were then submitted to hydrothermal treatment at 90 °C during 18 h for Zn_3AlCO_3 and 68 h for Zn_2AlCO_3 . The products were washed and dried in an oven at 60 °C. These samples will be designated as Zn_2AlVC and Zn_3AlVC .

Characterization. Zn, Al, and V elemental chemical analyses were obtained using atomic absorption spectroscopy after dissolution of the solid in 0.1 M HCl (Perkin-Elmer model 3100). Powder X-ray diffraction (PXRD) patterns were recorded with a Philips APD 1700 instrument, using Ni-filtered $\text{Cu K}\alpha$ radiation. The FT-IR spectra were obtained using a Nicolet 250 spectrometer in the 4000–400 cm^{-1} range, with a nominal resolution of 2 cm^{-1} and averaging 100 scans; the sample was dispersed in solid KBr. Specific surface area and porosity data were determined using an ASAP 2000 apparatus from Micromeritics. Samples were degassed previously in situ at 200 °C for 2 h. Thermogravimetric analysis curves (TG) were recorded in a Polymer Laboratory TG1500 apparatus in air, at a heating rate of 10 °C/min. Microstructural characterization of the material was carried out using a JEOL 200CX TEM.

X-ray absorption (XAS) data were collected on station 8.1 at the Daresbury Synchrotron Radiation Source (Daresbury, Warrington, U.K.) with an electron ring running at 2 GeV and 210–230 mA. Monochromatization was obtained with a bent double silicon crystal monochromator working at the (111) reflection. The crystals are bent in order to match the vertical dispersion of the source, hence eliminating the requirement of vertical defining slits to maintain the resolution. The monochromator was detuned 30% of its intensity to minimize the presence of higher harmonics. A well-defined small peak in the main edge jump of a V foil indicated an energy resolution better than 1 eV at the V K-edge. The measurements were carried out at 77 K in

Table 1. Elemental Chemical Analysis Data (Metals) and Specific Surface Areas for Parent Materials

sample	Zn ^a	Al ^a	Zn/Al ^b	c ^c	a ^c	S _{BET} ^d
Zn1AlCl	28.0	11.1	1.0	23.01	3.06	45
Zn2AlCl	34.7	6.7	2.1	23.24	3.08	21
Zn3AlCl	38.2	4.9	3.2	23.38	3.09	38
Zn4AlCl	39.2	3.9	4.1	23.45	3.10	24
Zn2AlCO ₃	35.0	7.0	2.1	22.91	3.07	21
Zn3AlCO ₃	38.4	5.2	3.1	22.97	3.08	25

^a % weight. ^b Atomic ratio. ^c Å. ^d $\text{m}^2 \text{g}^{-1}$.

transmission mode using optimized ion chambers as detectors. Samples were ground, diluted with boron nitride, and pressed into self-supported wafers with total absorbance ca. 2.5 just above the V K-edge, with V K-edge jumps being in the range 0.6–1.0. At least three scans were recorded and averaged in order to obtain the experimental spectra. Spectra for the crystalline compounds Na_3VO_4 , KVO_3 , and hexakis-(*n*-hexylammonium) decavanadate dihydrate were obtained by the same procedure. Sodium orthovanadate and potassium metavanadate were commercial from Alfa, while crystalline decavanadate was kindly provided by Roman et al.¹¹

The EXAFS function ($\chi(k)$) was obtained from the experimental X-ray absorption spectrum by conventional procedures.¹² Coordination parameters were obtained by best fit using experimental backscattering amplitude and phase shift functions for V–O absorber–backscatterer pairs obtained from the EXAFS spectrum of bulk Na_3VO_4 (four V–O bonds at 1.69 Å).¹³ The FEFF code^{14a} was used to obtain phase shifts and backscattering amplitudes for V–V absorber–backscatterer pairs. Fits were obtained using unfiltered data in k ($\Delta k = 3.4\text{--}11.1 \text{ Å}^{-1}$) and R ($\Delta R = 0\text{--}4 \text{ Å}$) space and proved to be good when working either with k^1 - or k^3 -weighting schemes. EXAFS data analysis and handling were performed by using the program package XDAP.^{14b}

Results and Discussion

Parent Materials. Results of chemical analyses for metals are given in Table 1. The Zn/Al atomic ratios in the coprecipitated solids (chloride and carbonate) are close to the solution values. LDHs containing Zn (e.g., Zn and Al or Zn and Cr) are usually prepared by the salt-oxide (ZnO) method,¹ but in such a case the $\text{Zn}^{\text{II}}/\text{M}^{\text{III}}$ atomic ratio is usually close to 2, whatever the atomic ratio in the starting solutions. To prepare LDHs with a different Zn/Al ratios the coprecipitation method has been used here.

The PXRD patterns for Zn_2AlCl and Zn_3AlCl are shown in Figure 1A. These patterns are characteristic of layered materials with a hydrotalcite-like structure. The presence of sharp and symmetric peaks indicates that the materials are well crystallized. Indexing is based on rhombohedral symmetry (polytype 3R₁).¹⁵ The lattice parameter values are given in Table 1 with the a value calculated from the position of the 110 reflection and the relationship $a = 2d(110)$.² The c parameter was calculated as three times the spacing corresponding to planes (003), leading to an average value of 23.3 Å. This corresponds to a gallery height of 2.9 Å, assuming a thickness of 4.8 Å for the cationic sheets, and is in good agreement with literature data for chloride-containing LDHs.²

The PXRD patterns for samples Zn_2AlCO_3 and Zn_3AlCO_3 are given in Figure 1B. These also show sharp, symmetric,

- (11) Roman, P.; Aranzabe, A.; Luque, A.; Gutierrez-Zorrilla, J. M. *Mater. Res. Bull.* **1991**, 23, 731.
- (12) Sayers, D. E.; Bunker, B. A. In *X-ray Absorption: Principles of EXAFS, SEXAFS and XANES*; Koningsberger, D. C., Prins, R., Eds.; Wiley: New York, 1988.
- (13) Tillmanns, E.; Baur, W. H. *Acta Crystallogr.* **1971**, B27, 2124.
- (14) (a) Mustre de Leon, J.; Rehr, J. J.; Zabinsky, S. I.; Albers, R. C. *Phys. Rev. B* **1991**, 44, 4146. (b) A complete description of this program package can be found in <http://www.xs4all.nl>.
- (15) Bookin, A. S.; Drifts, V. A. *Clays Clay Miner.* **1993**, 4, 551.

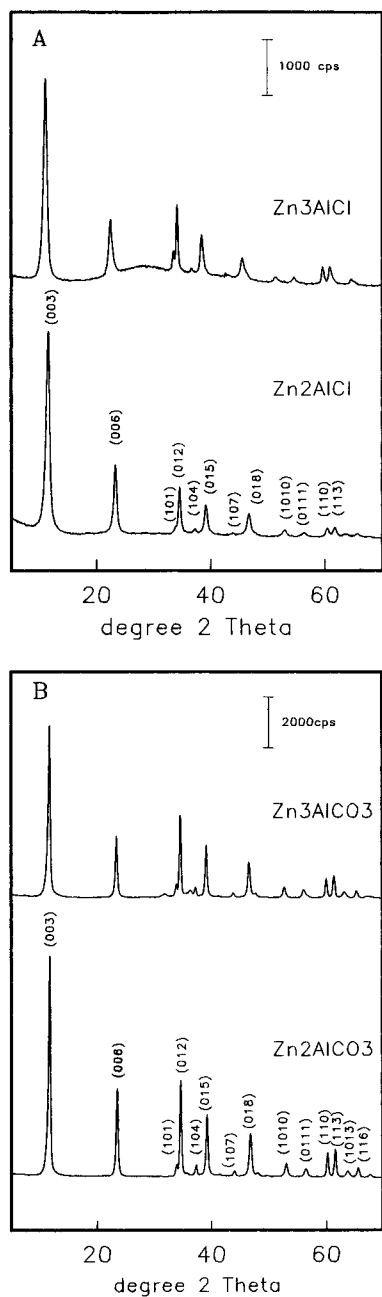


Figure 1. (A) PXRD patterns of samples ZnAlCl with Zn/Al ratios 2 and 3. (B) PXRD patterns of samples ZnAlCO₃ with Zn/Al ratios 2 and 3.

and intense peaks, due to well-crystallized materials. The values for parameters a and c , also given in Table 1, are within the range reported in the literature² for carbonate-containing hydrotalcite materials. The sharp and symmetric peaks are characteristic, according to Thevenot et al.,¹⁶ of an arrangement of well-ordered sheets, while for samples with other cations, such as Mg–Al, Mg–Mn, Ni–Mn, etc., some of the peaks are broad.^{2,17,18}

The low specific surface areas shown by these samples (average 29 m²/g) indicate well-crystallized solids, in agreement with the PXRD patterns. All isotherms belong to type IV in

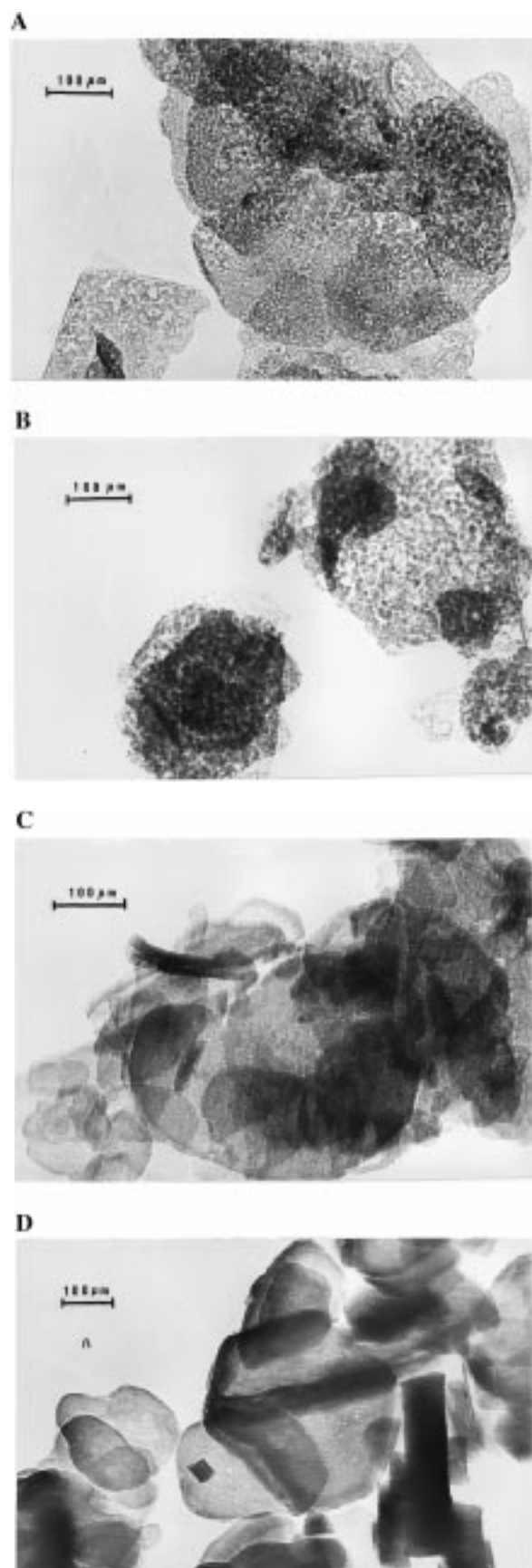


Figure 2. Transmission electron micrographs of samples (A) Zn₃AlCl, (B) Zn₂AlCO₃, (C) Zn₃AlV₇, and (D) Zn₂AlVC.

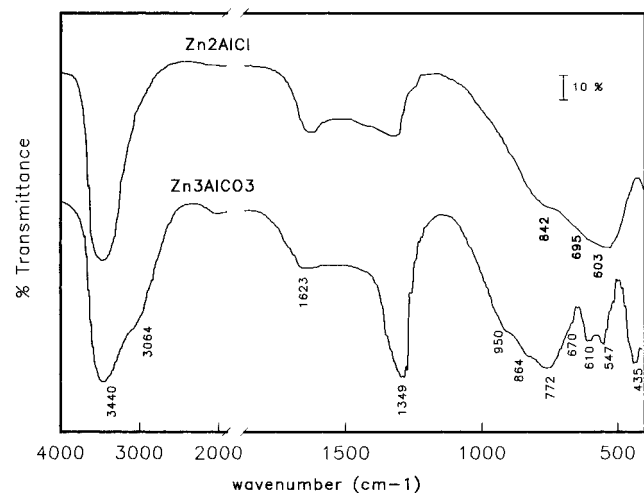
the IUPAC classification,¹⁹ characteristic of nonmicroporous materials, with an average pore diameter of 25 Å. During

- (16) Thevenot, F.; Szymanski, R.; Chaumette, P. *Clays Clay Miner.* **1989**, 37, 396.
- (17) Fernández, J. M.; Barriga, C.; Ulibarri, M. A.; Labajos, F. M.; Rives, V. *J. Mater. Chem.* **1996**, 4, 1117.
- (18) Barriga, C.; Fernández, J. M.; Ulibarri, M. A.; Labajos, F. M.; Rives, V. *J. Solid State Chem.* **1996**, 124, 205.

Table 2. Formulas and Water Content in the Parent Samples

formula	<i>n</i>	layer charge ^a density
[Zn _{0.512} Al _{0.488} (OH) ₂]Cl _{0.488}	0.51	0.060
[Zn _{0.679} Al _{0.321} (OH) ₂]Cl _{0.321}	0.68	0.039
[Zn _{0.763} Al _{0.237} (OH) ₂]Cl _{0.237}	0.92	0.029
[Zn _{0.811} Al _{0.189} (OH) ₂]Cl _{0.189}	1.15	0.023
[Zn _{0.675} Al _{0.325} (OH) ₂](CO ₃) _{0.166}	0.83	0.039
[Zn _{0.752} Al _{0.193} (OH) ₂](CO ₃) _{0.097}	nm	0.023

^a e Å⁻² following the method described in ref 21. nm: not measured.

**Figure 3.** FT-IR spectra of samples Zn₂AlCl and Zn₃AlCO₃.

adsorption at -196 °C, nitrogen molecules do not enter into the interlayer space, and so the measured surface area corresponds to the external surface of the particles. TEM micrographs for selected samples are shown in Figure 2. Platelike particles with hexagonal morphology are observed for all samples.

The TG curves for Zn₂AlCl and Zn₃AlCl show two weight losses at low temperature (ca. 130 and 230 °C) indicating the existence of two kinds of water in the interlayer space,^{20,21} i.e., water molecules held with different strengths. The dehydroxylation stage occurs at higher temperatures (400–600 °C), and chloride is removed as HCl above 600 °C.²² The TG curves for Zn₂AlCO₃ and Zn₃AlCO₃ show a continuous weight loss between 230 and 700 °C. The TG data allowed the amount of interlayer water to be calculated (Table 2). The layer charge density values, calculated by following the method by Pinnavaia et al.²¹ are also given in Table 2.

The FT-IR spectra of the samples differ only by the contribution of the interlayer anion. Two representative spectra are shown in Figure 3. The broad (as a result of hydrogen bonding) absorption in both spectra between 3600 and 3300 cm⁻¹ is due to the ν(OH) mode of the hydroxyl groups, both from the brucite-like layers and from interlayer water molecules. Interlayer water also gives rise to the broad, medium-intensity, absorption close to 1620 cm⁻¹, δ(H₂O). Hydrogen bonding of the water with interlayer carbonate anions^{23,24} also gives rise to a shoulder at 3064 cm⁻¹ in the spectrum of sample

Table 3. Elemental Chemical Analysis Data (Metals) and Specific Surface Areas for Pillared Compounds

sample	Zn ^a	Al ^a	V ^a	Zn/Al ^b	S _{BET} ^c
Zn ₂ AlV ₄	20.0	5.6	30.3	1.5	32
Zn ₂ AlV ₅	20.9	5.4	30.0	1.6	35
Zn ₂ AlV ₆	24.2	5.2	30.2	2.0	38
Zn ₃ AlV ₄	18.5	6.3	33.4	1.2	33
Zn ₃ AlV ₅	28.4	5.0	31.6	2.3	38
Zn ₃ AlV ₆	29.1	3.7	26.4	3.2	34
Zn ₃ AlV ₇	30.5	4.0	22.2	3.1	43
Zn ₂ AlVC	24.4	5.8	32.4	1.8	21
Zn ₃ AlVC	29.0	5.3	22.6	2.2	15

^a % weight. ^b Atomic ratio. ^c m² g⁻¹.

Zn₃AlCO₃. The very intense absorption at 1349 cm⁻¹ in the spectrum of this sample is due to mode ν₃ of the carbonate species. Absorptions below 800 cm⁻¹ are due to lattice vibrations, involving metal–oxygen stretching modes and, in the case of sample Zn₃AlCO₃, also modes ν₂ (out-of-plane deformation) and ν₄ (in-plane bending) of carbonate at 864 and 670 cm⁻¹, respectively. The medium band close to 1350 cm⁻¹ in the spectrum of sample Zn₂AlCl is probably the result of carbonate impurities, most likely adsorbed onto the external surface of the particles.

Polyoxovanadate-Pillared Zn–Al LDHs. Chemical analysis data for these solids are summarized in Table 3. It seems that the pH of the system during V incorporation plays a major role in determining the final Zn/Al ratio. The ratio decreases from the value existing in the chloride precursors when exchange is performed at low pH but is maintained at pH = 6–7. These changes may be related to the different selective dissolution of Zn^{II} or Al^{III} during the exchange process. The acidities of these cations, as indicated by the charge-to-radius ratio, are 13.3 e²/Å for Al^{III} but 4.55 e²/Å for Zn^{II},²⁵ and so precipitation of Al^{III} will take place at lower pH than that of Zn^{II}.

With respect to the vanadium content, it decreases as the pH increases for samples prepared from Zn₃AlCl, while samples prepared from Zn₂AlCl show little variation in V content. It might be expected that an increase in V content would be observed as the Zn/Al ratio decreases, as more vanadium should enter into the interlayer space as a polyoxovanadate anion, to compensate for the increasing positive charge in the layers, due to the layer aluminum content. However, such a relationship does not necessarily hold since different polyoxovanadate species can be formed, for which the (q/V) ratio between their formal charge and the vanadium content does not remain constant: for example, q/V is 0.6 for V₁₀O₂₈⁶⁻ but 1 for V₄O₁₂⁴⁻ and (VO₃)_nⁿ⁻. The stability of these species changes markedly with pH,²⁶ and control of pH during exchange will lead to intercalation of different polyoxovanadate species. Moreover, low pH values, where decavanadate is the major species, would give rise to H_xV₁₀O₂₈^{x-6} species, with different (q/V) ratios.²⁶ Simultaneously, different pH values during exchange also lead to different Zn/Al ratios in the brucite-like layers.

PXRD diagrams for samples prepared at a given pH were similar, irrespective of the Zn/Al atomic ratio (2 or 3) in the starting chloride-containing LDH. The PXRD patterns of selected vanadium-containing solids are shown in Figure 4. Although the general patterns are more complex than those

- (19) Sing, K. S. W.; Everett, D. H.; Haul, R. A.; Moscou, W. L.; Pierotti, R.; Rouquerol, J.; Sieminska, J. *Pure Appl. Chem.* **1985**, 57, 309.
- (20) Wang, J.; Tiangm, Y.; Wang, R.; Clearfield, A. *Chem. Mater.* **1992**, 4, 1276.
- (21) Yung, S. K.; Pinnavaia, T. J. *Chem. Mater.* **1995**, 7, 348.
- (22) De Roy, A.; Vernay, A. M.; Besse, J. P.; Thomas, G. *Analysis* **1988**, 16, 409.
- (23) Bish, D. L.; Brindley, G. W. *Am. Mineral.* **1977**, 62, 458.
- (24) Krüssink, E. C.; van Reijden, E. C.; Ross, L. L.; J. R. H. *J. Chem. Soc., Faraday Trans. 1* **1981**, 77, 649.

- (25) Huheey, J. E.; Keiter, E. A.; Keiter, R. L. In *Inorganic Chemistry. Principles of Structure and Reactivity*, 4th ed.; Harper Collins: New York, 1993.
- (26) Clark R. J. H.; Brown D. *The Chemistry of Vanadium; Niobium and Tantalum*; Comprehensive Inorganic Chemistry, Pergamon Texts in Inorganic Chemistry, Vol. 20, Pergamon Press: Oxford, U.K., 1973.

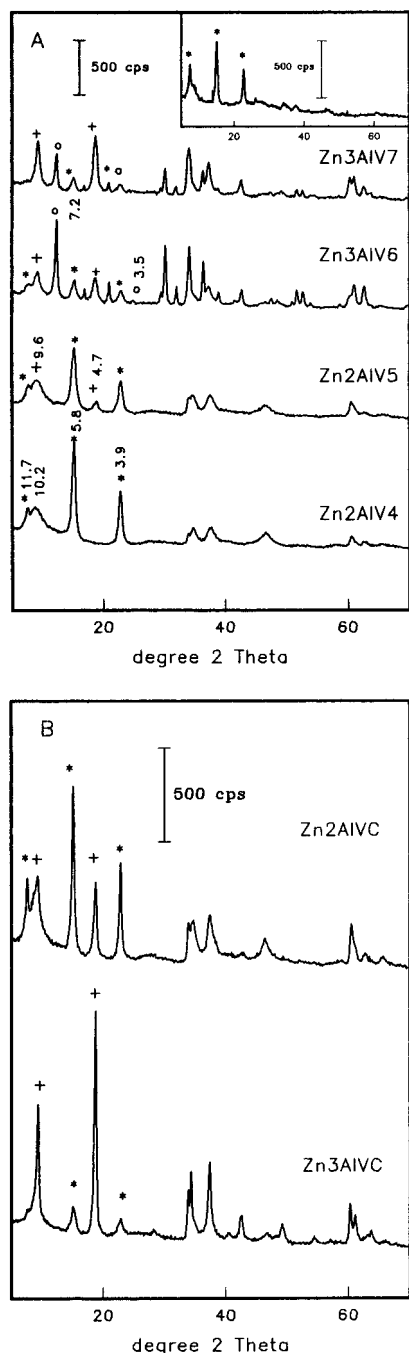


Figure 4. (A) PXRD patterns of vanadium-containing samples prepared at different pH values (see text): (*) peaks corresponding to (00*l*) planes of phases with $V_{10}O_{28}^{6-}$; (+) $V_4O_{12}^{4-}$; (O) $(VO_3)_n^{n-}$ interlayer anion. (B) PXRD patterns of the pillared samples from $ZnXAlCO_3$. Inset: PXRD pattern for sample Zn2AlIV4 recorded by following the oriented aggregate method.

shown in Figure 1 for the parent LDHs samples, they still correspond to layered materials. In particular, in some cases it appears that more than one layered phase exists. In all cases, indexing the patterns is on the basis of a rhombohedral symmetry.

The PXRD pattern for sample Zn2AlIV4 shows (00*l*) harmonics at 11.7, 5.8, and 3.9 Å, corresponding to a basal spacing $d(003)$ of 11.7 Å. Taking into account the thickness of the brucite-like layers, this spacing corresponds to a gallery height of 6.9 Å, a value matching that ascribed in the literature^{3,9} to interlayer $V_{10}O_{28}^{6-}$, a species with its main C_2 axis parallel to the brucite-like layers. The broad feature centered at 10.2 Å has been previously reported⁵⁻⁷ for samples similar to those

described here and has been ascribed to a byproduct, such as a metal salt of the polyoxovanadate formed during the exchange process (probably $Na_6V_{10}O_{28} \cdot 18H_2O$ which exhibits a PXRD pattern with several reflections within this 2θ range).²⁷ To confirm further the origin of this broad peak, the PXRD of this sample has been also recorded by following the oriented aggregate technique, leading to the profile inset in Figure 4A. This technique permits ordering of the platelike crystals of the layered sample, thus leading to enhanced intensity of the (00*l*) diffraction peaks, with respect to those produced by nonbasal planes. As it can be seen in the inset, the intensities of the three harmonics are enhanced, while that of the broad reflection at 10.2 Å decreases, thus confirming the origin of the former ones as due to a layered material with $c = 35.1$ Å and that the solid responsible for the reflection at 10.2 Å is not likely to be a layered material.

An apparently similar behavior is observed for Zn2AlIV5. Again, a series of harmonics is recorded in the PXRD diagram at 11.7, 5.8, and 3.9 Å that can clearly be ascribed to the presence of the layered material with $c = 35.1$ Å and decavanadate species in the interlayer (spacing 11.7 Å, gallery height 6.9 Å). The "broad reflection" close to 10.2 Å has now shifted to 9.6 Å, and in addition, a second weak reflection is recorded at 4.7 Å. These results suggest the presence of two layered phases, one as mentioned above containing decavanadate $V_{10}O_{28}^{6-}$ in the interlayer and the other with $c = 28.8$ Å (spacing = 9.6 Å, gallery height = 4.8 Å), which may be ascribed to the presence of $V_4O_{12}^{4-}$ species in the interlayer.^{3,28}

The PXRD pattern for Zn2AlIV6 is rather complex, although harmonics corresponding to several layered materials can be identified; the peak originally ascribed to planes (006) of the decavanadate-containing material at 5.8 Å is now rather weak, although detectable, as well as those due to the sample presumably containing $V_4O_{12}^{4-}$ in the interlayer (at 9.6 Å). However, the strongest peak in this diffractogram is now at 7.2 Å, with a second harmonic at 3.6 Å. These were not observed in the two patterns previously discussed. This spacing for planes (003) corresponds to a gallery height of 2.4 Å and results from a layered material containing chainlike polymeric vanadate $(VO_3)_n^{n-}$ anions.²⁸ Formation of such a species has been already claimed in LDHs containing Ni^{II} and Al^{III} in the layers^{6b} and also during thermal decomposition of decavanadate-containing Mg–Al hydrotalcite.²⁹

Finally, the pattern for the sample prepared at pH = 7 shows a lower number of peaks, which may be ascribed to harmonics of biphasic (both layered) materials, characterized by (003) spacings at 9.6 and 7.2 Å.

The PXRD patterns for the polyoxovanadate-containing LDHs prepared from carbonate-containing samples are shown in Figure 4B. Overall, the samples are more crystalline (sharper and more intense PXRD peaks) than those obtained from the chloride-containing samples. This difference may be due to a favored crystallization because of a higher reaction temperature (60 °C instead of 40 °C) during preparation of the ex-carbonate samples. Two crystalline phase are observed for sample Zn2AlIVC, with $d(003)$ harmonics at 11.7 and 9.6 Å, possessing similar intensities. For sample Zn3AlIVC, the major phase is that associated with the (003) harmonic at 9.6 Å, the other phase $V_{10}O_{28}^{6-}$, with (003) harmonic at 11.7 Å, being only a minor component.

(27) JCPDS, Joint Committee on Powder Diffraction Standards. *Powder Diffraction File*; International Centre for Diffraction Data: Swarthmore, PA, 1977.

(28) Twu, J.; Dutta, P. K. *J. Phys. Chem.* **1989**, 93, 7863.

(29) Kooli, F.; Crespo, I.; Barriga, C.; Ulibarri, M. A.; Rives V. J. *Mater. Chem.* **1996**, 6, 1199.

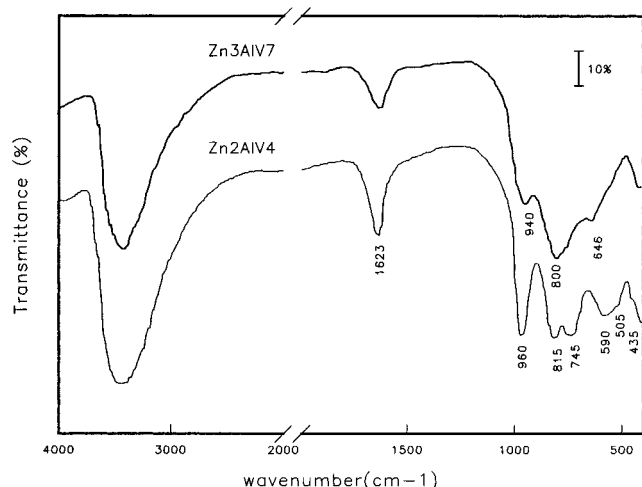


Figure 5. FT-IR spectra of vanadium-containing samples prepared at pH 4 and 7.

The FT-IR spectra of two representative polyoxovanadate-containing samples prepared from chloride samples are shown in Figure 5. The spectrum for Zn2AlV4 (for which PXRD suggests $V_{10}O_{28}^{6-}$ as the interlayer species) is very similar to that previously reported^{4,30,31} for decavanadate-containing LDHs. The broad absorption at 3800–3400 cm^{-1} is due to $\nu(\text{OH})$ of hydroxyl groups (from the layers and the water molecules), while the medium-intensity band at 1623 cm^{-1} is due to mode $\delta(\text{H}_2\text{O})$. The bands at 960, 815, 745, 598, and 505 cm^{-1} have also been previously attributed to decavanadate species in the gallery. For sample Zn3AlV7 some bands are much broader, probably due to the coexistence of two different polyoxovanadate species. The band at 940 cm^{-1} can be assigned to symmetric mode $\nu_{\text{V=O}}$, and the 646 cm^{-1} band is attributed to $\nu_{\text{V-O}}$ in bridging V–O–V units in a tetrahedral chain.³⁰ The spectrum of sample Zn3AlV7 is almost identical to that of sample Zn3AlV4 shown in Figure 5.

The specific surface area values for the vanadate materials are of the same order as those of the parent samples (Table 3), indicating that the nitrogen molecules do not enter into the interlayer space that has been expanded in the vanadate-containing samples. However, pore size distributions are wider (50–110 Å), and the average pore diameter has increased (35 Å). The nitrogen adsorption–desorption isotherms correspond to type IV in the IUPAC classification.¹⁹

Transmission electron micrographs for selected vanadate-exchanged samples are shown in Figure 2c,d; the shape of the original hexagonal crystallites is not affected by exchange.

EXAFS oscillations at the V K-edge for samples obtained by anionic exchange of a chloride precursor at pH = 4, 5, 6, and 7 are shown in Figure 6. Associated k^3 -weighted Fourier transforms (FTS) and V K-XANES spectra for the same samples are plotted in Figures 7 and 8, respectively, which also include XAS data for selected reference compounds (Na_3VO_4 , KVO_3 , and hexakis(*n*-hexylammonium) decavanadate). The whole XANES and EXAFS spectra recorded for sample Zn2AlV4 are almost identical to those obtained for crystalline decavanadate. k^3 -weighted FTs associated with their V K-EXAFS oscillations showing two overlapped low intensity peaks at $R < 2$ Å and an intense peak at 2.3 Å. Therefore, XAS data clearly identify $V_{10}O_{28}^{6-}$ anions as the species responsible for a basal spacing

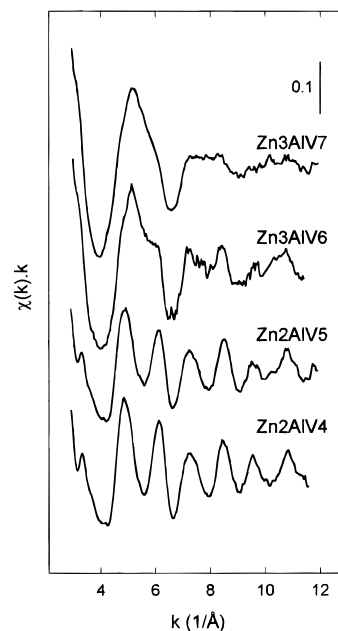


Figure 6. V K-edge EXAFS oscillations for samples obtained from a ZnXAlCl precursor.

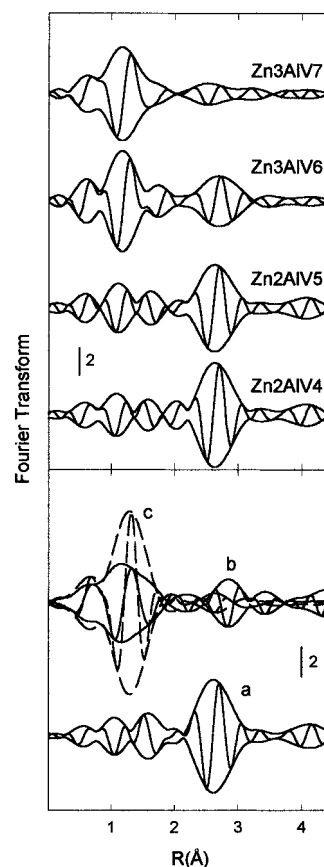


Figure 7. Modulus and imaginary part of the k^3 -weighted Fourier transforms associated with V K-EXAFS. Top panel: samples obtained from a ZnXAlCl precursor. Bottom panel: selected reference compounds of (a) crystalline decavanadate, (b) KVO_3 , and (c) Na_3VO_4 ($\Delta k = 3.4$ – 11.5 Å^{−1} in all the Fourier transforms).

of 11.7 Å, the only layered phase detected by PXRD in this sample. Reasonable coordination parameters for V^{5+} cations in decavanadate anions are obtained by best fit of their V K-EXAFS oscillations. Fit results for a model (Table 4) with

(30) Lopez-Salinas, E.; Ono, Y. *Bull. Chem. Soc. Jpn.* **1992**, 65, 2465.

(31) Kooli, F.; Rives, V.; Ulibarri, M. A. *Mater. Sci. Forum* **1994**, 152, 375.

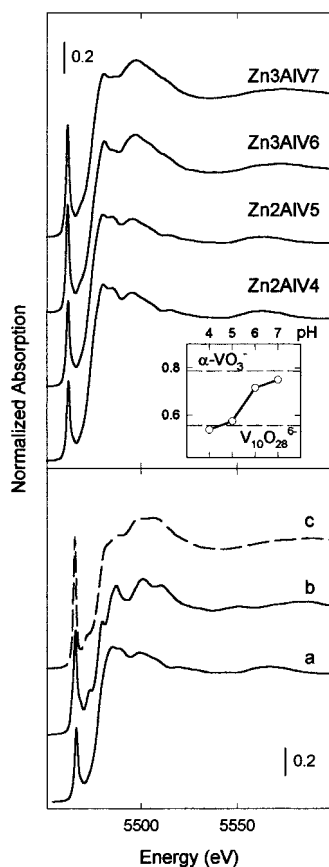


Figure 8. V K-XANES spectra. Top panel: samples obtained from a ZnXAlCl precursor. Bottom panel: selected reference compounds of (a) crystalline decavanadate, (b) KVO₃, and (c) Na₃VO₄. Inset: intensity of the pre-edge peak vs the pH of synthesis; dashed lines indicate intensity values for α -VO₃⁻ chains and decavanadate anions in reference compounds.

two average V–O bond lengths and a single V–V shell are plotted in Figure 9A,B for bulk decavanadate and sample Zn2AlV4, respectively. The total V–O coordination number (5.4–5.9) and bond lengths (V–O₁ = 1.61 Å, V–O₂ = 1.85 Å) obtained from EXAFS are in agreement with those expected for the structure of decavanate anions (Chart 1), where V⁵⁺ cations are in a very distorted octahedral coordination, crystallographic data¹¹ yielding an average oxygen coordination number of 5.0 up to 2.1 Å grouped in short (1.589–1.682 Å) and medium (1.787–2.105 Å) distances. Longer distances (2.141–2.374 Å) that complete the octahedral coordination in the cluster are missed in our fit. Meanwhile, V–V shell radii from EXAFS data (3.09 Å) coincide, within the experimental error, with the average bond length expected in the 3–4 Å range (3.12 Å),¹¹ although the coordination number from EXAFS (2.3) is clearly lower than the expected one (4.8 from crystallographic data).

The pH of the exchange solution clearly influences the local structure around vanadium cations existing in the interlayer space. In the XANES region (Figure 8) changes in the pre-edge peak position are negligible, indicating that in all samples vanadium cations are in the +5 oxidation state, but the intensity of the pre-edge peak increases with pH, with post-edge features also showing significant changes. Pre-edge peak intensities for samples prepared at pH = 6–7 are similar to that found for KVO₃, where tetrahedral [VO₄] units share a vertex forming an infinite chain (Chart 1).³² This fact suggests that, in samples synthesized at high pH values, interlayer species are mainly

Table 4. Fit Parameters at the V K-Edge for Hexakis(*n*-hexylammonium) Decavanadate Dihydrate and for Zn–Al–Vanadate Hydrotalcite Samples^a

shell	<i>N</i>	10 ³ Δσ ² (Å) ²	<i>R</i> (Å)	Δ <i>E</i> ^o (eV)
V ₁₀ O ₂₈ ⁶⁻				
O	2.0	6.5	1.61	1.5
O	3.9	10.5	1.85	5.2
V	2.3	1.8	3.09	12.6
Zn2AlV4				
O	2.0	6.0	1.61	4.7
O	3.4	10.3	1.85	6.1
V	2.3	1.8	3.09	12.6
Zn2AlV5				
O	2.1	4.2	1.63	−2.7
O	2.7	7.1	1.87	5.4
V	2.0	1.8	3.10	12.0
Zn3AlV6				
O	2.8	1.7	1.67	−2.0
O	1.7	1.4	1.87	−0.2
V	1.3	1.8	3.14	7.2
Zn3AlV7				
O	2.8	1.7	1.67	−2.0
O	1.7	1.1	1.83	4.6
V	0.5	1.8	3.10	12.4
Zn2AlVC				
O	1.8	8.5	1.63	4.7
O	2.9	14.6	1.85	6.1
V	2.1	1.8	3.09	12.6
Zn3AlVC				
O	2.8	4.4	1.67	−0.9
O	1.4	1.3	1.84	5.1
V	0.7	1.8	3.07	20.0

^a Estimated errors for coordination numbers (*N*) and bond lengths (*R*) are ±10% and ±0.02 Å, respectively.

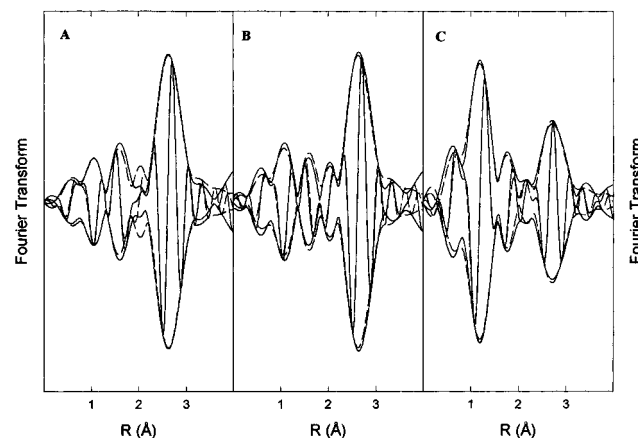
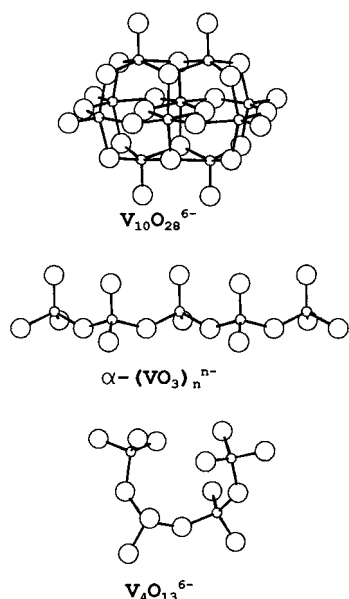


Figure 9. Experimental *k*³-weighted Fourier transforms (solid lines) and best fit functions (dashed lines; fit range Δ*k* = 3.5–11.1 Å^{−1}) for hexakis(*n*-hexylammonium) decavanadate dihydrate (A) and for hydrotalcite samples obtained from a ZnXAlCl precursor at pH = 4 (B) and pH = 6 (C).

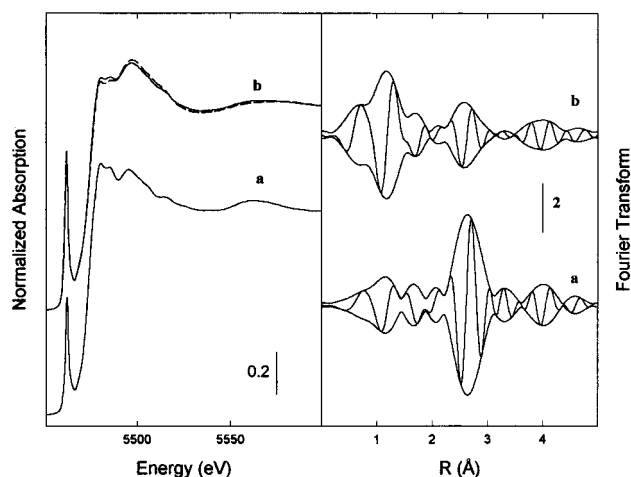
formed by [VO₄] units sharing vertex. EXAFS data confirm this conclusion: When the pH is increased, the intensity of the maximum at low *R* increases (Figure 7), while that of the maximum at 2–3 Å decreases. EXAFS spectra recorded for samples Zn3AlV6 and Zn3AlV7 are also similar to that recorded for bulk KVO₃. Best fit parameters for these samples are summarized in Table 4, while Figure 9C shows experimental data and best fit functions for Zn3AlV6. The extensive formation of polyvanadates with [VO₄] units leads to a decrease

(32) Hawthorne, F. C.; Calvo, C. J. *Solid State Chem.* **1977**, 22, 157.

Chart 1. Structure of Vanadate Anions (Large Circles, Oxygen Atoms; Small Circles, Vanadium Atoms)

in the total oxygen coordination number from 5.4 for Zn2AlV4 to 4.5 for Zn2AlV6 and Zn2AlV7. As described above, PXRD indicated that sample Zn3AlV7 was a mixture of phases, major components having (003) basal spacings of 9.6 and 7.2 Å associated with $V_4O_{12}^{4-}$ and metavanadate chains, respectively.^{3,28} In agreement with this interpretation, XAS data confirm that vanadates yielding these basal spacing are formed by tetrahedral $[VO_4]$ units. Also in agreement with XRD results, EXAFS coordination parameters for sample Zn2AlV5 indicate an intermediate situation where tetrahedral vanadates coexist with decavanadate clusters. Meanwhile, the V–V coordination number steadily decreases as the synthesis pH increases, suggesting a lower polymerization degree of $[VO_x]$ polyhedra than that found in the decavanadate cluster.

X-ray absorption data for samples obtained from carbonate-containing precursor are summarized in Figure 10. The XANES spectrum for sample Zn2AlVC can be ascribed to decavanadate species, while the best fit of EXAFS data yield V–O and V–V coordination numbers (Table 4) slightly lower than those determined for crystalline decavanadate. In agreement with PXRD data, these results indicate that $V_{10}O_{28}^{6-}$ is the main interlayer species in this sample, and only a fraction of vanadate anions are formed by tetrahedral $[VO_4]$ units. On the other hand, the best fit parameters in Table 4 for sample Zn3AlVC are typical of anions formed by $[VO_4]$ units. As reported above, PXRD indicates that the main phase present in this sample has an interlayer space of 9.6 Å, previously associated with the presence of $V_4O_{12}^{4-}$.³ Tetravanadate anions in aqueous solution have been described²⁶ as formed by four $[VO_4]$ units which share a vertex in a cyclic structure, and therefore, the expected local order around V^{5+} cations in this anion is identical to that described for $\alpha-VO_3^-$ chains with four oxygen neighbors at short (1.6 Å) and long (1.8 Å) distances accounting for terminal V–O and bridging V–O–V bonds.³² A tetravanadate anion with an open ring structure (see Chart 1), which could be described as a four-member $\alpha-VO_3^-$ chain, is in fact found in $Ba_3V_4O_{13}$.³³ Although V K-EXAFS data for Zn3AlVC are consistent with the presence of tetravanadate species, accounting for a basal

**Figure 10.** V K-XANES spectra (left panel) and modulus and imaginary part of the k^3 -weighted Fourier transforms associated to the EXAFS oscillations (right panel; $\Delta k = 3.4\text{--}11.9\text{ \AA}^{-1}$) for samples obtained from a Zn_2AlCO_3 (a) and Zn_3AlCO_3 (b) precursors. The dashed line accounts for the corrected XANES spectrum of tetravanadate species after subtracting the decavanadate component (see text).

spacing of 9.6 Å, first-shell coordination parameters are similar for $\alpha-VO_3^-$, suggested to yield a basal spacing of 7.2 Å.²⁸ Therefore, EXAFS seem to be unable to distinguish between both species. The systematic underestimation of V–V coordination numbers, reported above for decavanadate clusters, and the constant value of V–V distances in all the samples here studied ($3.10 \pm 0.04\text{ \AA}$) prevent us from providing a clue about the chain length of the interlayer species from these data.

Characteristic features for the species responsible for the basal spacing 9.6 Å appear in the XANES region of the V K-XAS. In fact, theoretical studies³⁴ have shown that spectral features in the near-edge region are sensitive to the cluster structure up to ca. 5 Å. Unlike EXAFS oscillations, XANES features are sensitive not only to shell distances but also to bond angles, and it is reasonable to expect differences between the near-edge fine structure for $\alpha-VO_3^-$ chains and tetravanadate clusters forming either open or closed rings. Comparison of the XANES spectrum for Zn3AlVC (Figure 10, trace b) with that recorded for KVO_3 (Figure 8, trace b) shows that preedge peak intensities are similar (0.75 and 0.79, respectively), as expected from the presence in both cases of similarly distorted $[VO_4]$ units, but postedge features are clearly different. The spectrum recorded for Zn3AlVC also differs in preedge peak intensities and in the postedge fine structure, compared to those obtained for other tetrahedral vanadates such as Na_3VO_4 or compounds containing the anion $V_2O_7^{4-}$.^{35,36} Following the previous assignment of the basal spacing 9.6 Å to the presence of $V_4O_{12}^{4-}$, the XANES spectrum of Zn3AlVC is assigned to tetravanadate species. In agreement with the PXRD data, this seems to be the major component in this sample, with only a minor contamination by the decavanadate intercalate.

At this point we know the characteristic V K-XANES spectra of two vanadate species existing in the interlayer (decavanadate, interlayer spacing 11.7 Å; tetravanadate, interlayer spacing 9.6 Å). Experimental XANES data, $X\mu(E)$, shown in Figure 8 for

(33) Gatehouse, M. M.; Guddat, L. W.; Roth, R. S. *J. Solid State. Chem.* **1987**, 71, 390.

(34) Ruiz-López, M. F.; Muñoz-Páez, A. *J. Phys.: Condensed Matter* **1991**, 3, 8981.

(35) Del Arco, M.; Rives, V.; Trujillano, R.; Malet, P. *J. Mater. Chem.* **1996**, 6, 1419.

(36) Del Arco, M.; Galiano, M. V. G.; Rives, V.; Trujillano, R.; Malet, P. *Inorg. Chem.* **1996**, 35, 6362.

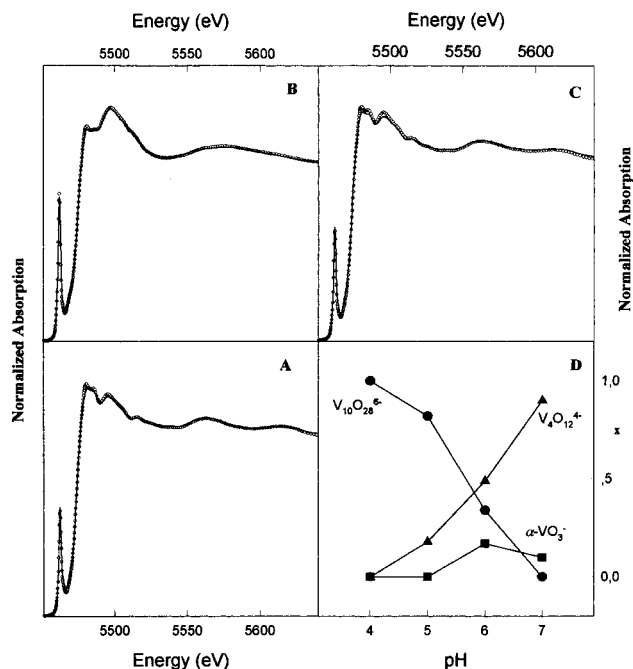


Figure 11. Experimental V K-XANES spectra (dots) and best fit functions (lines) obtained by considering mixtures of vanadate species (see text): (A) Zn2AlV4; (B) Zn3AlV7; (C) Zn2AlVC; (D) fraction of V^{5+} cations as $V_{10}O_{28}^{6-}$, $V_4O_{12}^{4-}$, and $\alpha\text{-VO}_3^-$ for samples obtained from a ZnXAlCl precursor.

samples Zn2AlV4 and Zn2AlV5 and those shown in Figure 10 for sample Zn2AlVC, can be fitted by considering the following equation:

$$X\mu(E) = aX\mu(E)_{\text{decavanadate}} + bX\mu(E)_{\text{tetravanadate}} \quad (1)$$

Parameters a and b were optimized by least-squares fitting and provide a quantitative estimation of the fraction of vanadium cations in each interlayer species, although we cannot forget the uncertainty arising because of the presence of vanadium-containing byproducts. In agreement with PXRD data, XANES data for sample Zn2AlV4 are best fitted (Figure 11A) with $a = 1.00 \pm 0.01$ and $b = 0.00 \pm 0.01$, indicating that only the decavanadate intercalate is present. Data for Zn2AlV5 (not shown) and those for Zn2AlVC (Figure 11C) are best fitted with $a = 0.76 \pm 0.03$, $b = 0.24 \pm 0.03$ and $a = 0.83 \pm 0.02$, $b = 0.18 \pm 0.02$, respectively, showing that in both cases a mixture of phases is obtained.

PXRD data for samples Zn3AlV6 and Zn3AlV7 indicated the presence of another phase with basal spacing of 7.2 Å, previously ascribed to the presence of $\alpha\text{-VO}_3^-$ chains.²⁸ In fact, best fit of XANES data for these samples is obtained by using the following expression:

$$X\mu(E) = aX\mu(E)_{\text{decavanadate}} + bX\mu(E)_{\text{tetravanadate}} + cX\mu(E)_{\alpha\text{-chain}} \quad (2)$$

Here $X\mu(E)_{\alpha\text{-chain}}$ corresponds to the spectrum recorded for KVO_3 . The set of parameters ($a = 0.19 \pm 0.03$, $b = 0.64 \pm 0.03$, $c = 0.17 \pm 0.02$) for Zn3AlV6 agrees with the presence of three phases in this sample and confirms that the structure of the interlayer species responsible for the basal spacing of 7.2 Å is similar to that described for $(VO_3)_n^{n-}$ chains in KVO_3 .

A negative a value, however, is obtained for the sample Zn3AlV7 ($a = -0.28 \pm 0.02$, $b = 1.18 \pm 0.02$, $c = 0.10 \pm 0.01$), fit shown in Figure 11B. This is not surprising, since PXRD data suggest that the decavanadate species is a minor component in sample Zn3AlVC and, therefore, its XANES spectrum used in expressions (1) and (2), as characteristic of tetravanadate, should be "contaminated" with the spectrum of decavanadate. The negative a -value for sample Zn3AlV7 indicates a decavanadate content even lower in this case, and in fact, peaks in the diffraction pattern ascribed to the decavanadate intercalate are nearly absent in the PXRD diagram for this sample. Assuming that the decavanadate content is close to zero for sample Zn3AlV7, a corrected profile for the spectrum of the tetravanadate component can be obtained (Figure 10, dotted line) and fractions of the individual components can be recalculated. Figure 11D summarizes corrected fractions of vanadium cations as decavanadate, tetravanadate, and α -chains, as a function of the pH during anionic exchange for samples obtained from a ZnXAlCl precursors.

Concluding Remarks

The method described here has led to the synthesis of well-crystallized materials with the hydrotalcite structure. The nature of the interlayer oxovanadate species (and, thus, the interlayer spacing) depends on the pH during synthesis.

V K-XAS data, either in the EXAFS or XANES region, unambiguously identify decavanadate clusters, where vanadium cations are in distorted octahedral coordination, as responsible of the basal spacing 11.7 Å.

Increasing the pH value used in anionic exchange favors the formation of interlayer vanadates formed by tetrahedral $[VO_4]$ units. Coordination parameters obtained from EXAFS are similar for interlayer species yielding basal spacings of 9.6 and 7.4 Å and indicate that both are formed by vertex-sharing tetrahedral units.

Fine structure of the XANES region is sensitive to structural differences between the three interlayer species detected. Analysis of XANES data allowed us to obtain the characteristic spectrum of the interlayer species yielding a basal spacing 9.6 Å, previously assigned to tetravanadate.

Experimental XANES spectra for the set of hydrotalcites can be reproduced by adding three individual components, that obtained for tetravanadate and those recorded for crystalline decavanadate and bulk KVO_3 . These three components account for basal spacing 9.6, 11.7, and 7.2 Å, respectively. The procedure allows one to estimate fractions of vanadium in the form of each interlayer species, taking into account the difficulties arising when vanadate-containing byproducts are formed.

Acknowledgment. Financial support from the CICYT (Grant MAT93-0787), the DGYCYT (Grant PB92-0665), the Consejería de Educación y Cultura de la Junta de Castilla y León (ref. SA56/94), and the Junta de Andalucía (Grupo FQM214) is gratefully acknowledged. C.B. acknowledges a grant from the Universidad de Córdoba, Junta Andalucía, Spain, and also thanks Dr. F. Romero for measuring the specific surface areas of the samples. Thanks are given to the CLRC Daresbury Laboratory for provision of synchrotron radiation (Grants 23/56 and 25/358).

IC9709133